

Carbon Nanotubes Reinforced Nylon-6 Composite Prepared by Simple Melt-Compounding

Wei De Zhang,* Lu Shen, In Yee Phang, and Tianxi Liu*

*Institute of Materials Research and Engineering,
3 Research Link, Singapore 117602*

Received October 22, 2003

Revised Manuscript Received December 12, 2003

Because of their high aspect ratio, nanosize in diameter, very low density, and, more importantly, excellent physical properties (such as extremely high mechanical strength, high electrical and thermal conductivity),¹ carbon nanotubes (CNTs) have been considered as ideal reinforcing fillers in polymer nanocomposites with high performance^{2–4} and multifunctions.^{5–9} The challenges for developing high-performance CNTs/polymer nanocomposites are (i) homogeneous dispersion of CNTs in the polymeric matrix and (ii) strong interfacial interactions so as to effect efficient load transfer from the polymeric matrix to the CNTs. Without chemically bonding, load transfer between the CNTs and the matrix mainly comes from electrostatic and van der Waals interactions.¹⁰ Much efficiency of load transfer can be realized by chemical bonding of polymeric matrix with functionalized CNTs.^{11,12} It has been confirmed that refluxing CNTs with concentrated nitric acid creates acidic sites on CNTs, such as carboxylic, carbonyl, and hydroxyl groups.^{13–15} These reactive groups on CNTs will greatly enhance the combination of CNTs with polymeric matrix, thus improving the mechanical strength of the nanocomposites.¹⁶ Sidewall functionalization of CNTs also improves the dispersion of CNTs in a polymeric matrix.^{12,17,18} Several methods have been developed to prepare CNTs/polymer composites, e.g., solution-casting,^{19–22} melt-mixing,^{23,24} and in situ polymerization of monomers with presence of CNTs.^{25,26} With solution-casting method, high-energy sonication of the CNTs suspensions over prolonged periods of time^{20,21} or the use of ultrasonic head²² is usually necessary to produce uniformly dispersed CNTs suspensions before they are subsequently mixed with polymer solutions. The use of surfactants has been demonstrated to improve the dispersion and strengthen the interactions between the multiwalled carbon nanotubes (MWNTs) and the epoxy resin.²⁷

Some CNTs enhanced polymer composites have been prepared. Dickey and his colleagues reported that addition of 1 wt % nanotubes into polystyrene by a simple solution-evaporation method results in 36–42% and 25% increases in elastic modulus and break stress, respectively.²⁰ A fragmentation test under tensile stress on MWNTs/urethane–diacrylate oligomer indicated that the stress transfer efficiency of MWNTs/matrix to be at least 1 order of magnitude larger than in conventional fiber-based composites.²⁸ Windle et al. prepared the CNTs/poly(vinyl alcohol) composite films with a wide range of CNTs loadings (10–60 wt %) by mixing

aqueous poly(vinyl alcohol) solution with CNTs dispersions followed by subsequent casting and controlling evaporation.¹⁹ Bower et al. fabricated CNTs/poly(hydroxyamino ether) by solution-casting and studied the deformation of CNTs in the composites. They reported that the onset buckling strain and fracture strain were estimated to be 5% and >18%, respectively.²⁹ However, the improvement in mechanical properties of the reported polymer nanocomposites with small amounts of CNTs as fillers are usually limited, mainly due to formation of severe CNTs agglomeration and/or poor interfacial interaction with the matrix. To avoid the impediment of growing polymer chains due to the presence of CNTs, Jia et al. reported an improved in situ process to enhance the interfacial adhesion between CNTs and nylon-6 matrix; however, the improvement in mechanical properties is still very limited, by about 20%.³⁰ In this Communication, MWNTs/nylon-6 (PA6) nanocomposites have been successfully prepared by simple melt-compounding and show significant improvement in mechanical properties compared with neat PA6.

Polyamide 6 (PA6) pellets (Grade SF1080A) used in this study are a product of Ube Industries under license from Toyota. The MWNTs were prepared by catalytic chemical vapor deposition (CVD) of methane on Co–Mo/MgO catalysts,^{31,32} with MWNTs yield of about 600% according to catalyst weight.³³ The catalyst in the as-prepared sample was removed by dissolving in concentrated nitric acid, and then the carbon nanotube powder was filtered and washed with deionized water for at least five times. The MWNTs were further refluxed in 2.6 M nitric acid for increasing more carboxylic and hydroxyl groups.³⁴ PA6 composite containing 1 wt % MWNTs was prepared via a melt-compounding method using a Brabender twin-screw mixer at 250 °C for 10 min with a screw speed of 100 rpm. Film samples (with thickness of 0.5 mm) were prepared by compression-molding in a press at a temperature of 250 °C with a pressure of 150 bar, followed by quickly quenching in an ice/water bath. A field emission scanning electron microscope (SEM) (JEOL JSM 6700F) was used to observe the purified MWNTs and the morphology of the failure surfaces of the CNTs/PA6 composite. Transmission electron microscopy (TEM) observation of MWNTs was performed with a Philips CM 300 FEG instrument operated at 200 kV.

The quenched films were finally punched into dog-bone specimens with a dimension of 63.5 × 9.53 × 3.18 mm³ (Die ASTM D-638 type V) using a CEAST hollow die punch (model 6051). The tensile tests were carried out using an Instron universal material testing system (model 5567) at room temperature with gauge length of 25 mm and crosshead speed of 5 mm/min. Property values reported here represent averaged results for at least six specimens. The nanoindentation tests were performed on the MTS Nano Indenter XP with a continuous stiffness measurement (CSM) technique.³⁵ The stiffness data can be calculated from the frequency and phase angle, which allows hardness (*H*) and elastic modulus (*E*) of the material to be determined as a function of indentation depth with a single indentation loading/unloading cycle.³⁶ Typical experimental procedures were as follows: the indenter approached the surface until contact was detected; it was followed by a

* To whom correspondence should be addressed. Wei De Zhang: e-mail wd-zhang@imre.a-star.edu.sg; Tel +65-68741993; Fax +65-68720785. Tianxi Liu: e-mail liu-tx@imre.a-star.edu.sg; Tel +65-68748594; Fax +65-67744657.

loading segment with a constant strain rate of 0.05 1/s to maximum depth, i.e., 5000 nm in present study; the load at this maximum depth was held constant for 60 s; and then the indenter was withdrawn from the sample in the same rate as loading until 10% of the maximum load. A three-side pyramid (Berkovich) diamond indenter was employed. At least 10 indents were performed on each sample on different regions, and an interval of 50 μm was chosen between each two indents to avoid interaction.

Figure 1A shows the SEM image of the purified and acid-treated MWNTs prepared in our laboratory by catalytic CVD. One can see many tubes loosely entangled together without any particle-like impurities. The inset in Figure 1A shows the TEM image of a MWNT with defects (indicated by arrow) on the wall. These defects can provide useful sites for chemical or physical functionalization of CNTs.¹⁴ Figure 1B,C shows the fracture surfaces of the composite (containing 1 wt % MWNTs) after tensile test. The well-dispersed bright dots and lines are the ends of the broken MWNTs. SEM images clearly show that a homogeneous dispersion of MWNTs is achieved throughout the PA6 matrix. Moreover, close inspection indicates that upon failure most of the MWNTs were broken rather than just pulled out of the matrix. A nanotube, as indicated by arrow 1 in Figure 1C, was observed to be stretched out of the matrix surface with a curved and tapered end, while another end of the tube was still strongly embedded in the matrix. This interesting and typical breakage phenomenon of the CNTs upon tensile stretching indicates a strong interfacial adhesion between MWNTs and PA6 matrix. In addition, another beltlike CNTs was observed which interconnects two polymer lumps, as indicated by arrow 2. Obviously, this interconnection is realized by an individual tube or bundles of MWNTs wrapped by the matrix since it is much bigger than the others. Moreover, the middle part of the tube is smaller than the two ends adhered to the two lumps of polymeric matrix. This also indicates that the interconnection of MWNTs with PA6 matrix is very strong.

Typical stress-strain curves for neat PA6 and MWNTs/PA6 composite are shown in Figure 2A. A pronounced yield and postyield drop are observed for neat PA6, while there is almost no noticeable yield for MWNTs-reinforced PA6 composite. It can be seen that addition of MWNTs significantly improves the tensile properties of PA6 matrix, as summarized in Table 1. Upon incorporation of only 1 wt % MWNTs, the elastic modulus of PA6 is improved by about 115% from 396.0 to 852.4 MPa, and the tensile strength at yield is improved by about 124% from 18.0 to 40.3 MPa. The elongation at break (about 125%) slightly decreases, indicating that the composite becomes somewhat brittle compared with neat PA6 (which breaks at above 150% of elongation). In addition, it should be noted that both yield strength and modulus of PA6 are considerably lower than the values (for the injection-molded bulk specimens) previously reported in the literature.³⁷ This is probably due to (i) the quenched (amorphous) sheet samples used here and (ii) sample preparation by compression-molding. Generally, the tensile test results indicate that the mechanical properties of MWNTs/PA6 composite are substantially superior to those of neat PA6 probably due to (i) the reinforcement of finely dispersed high-performance MWNTs nanofillers throughout the polymeric matrix and (ii) strong interaction

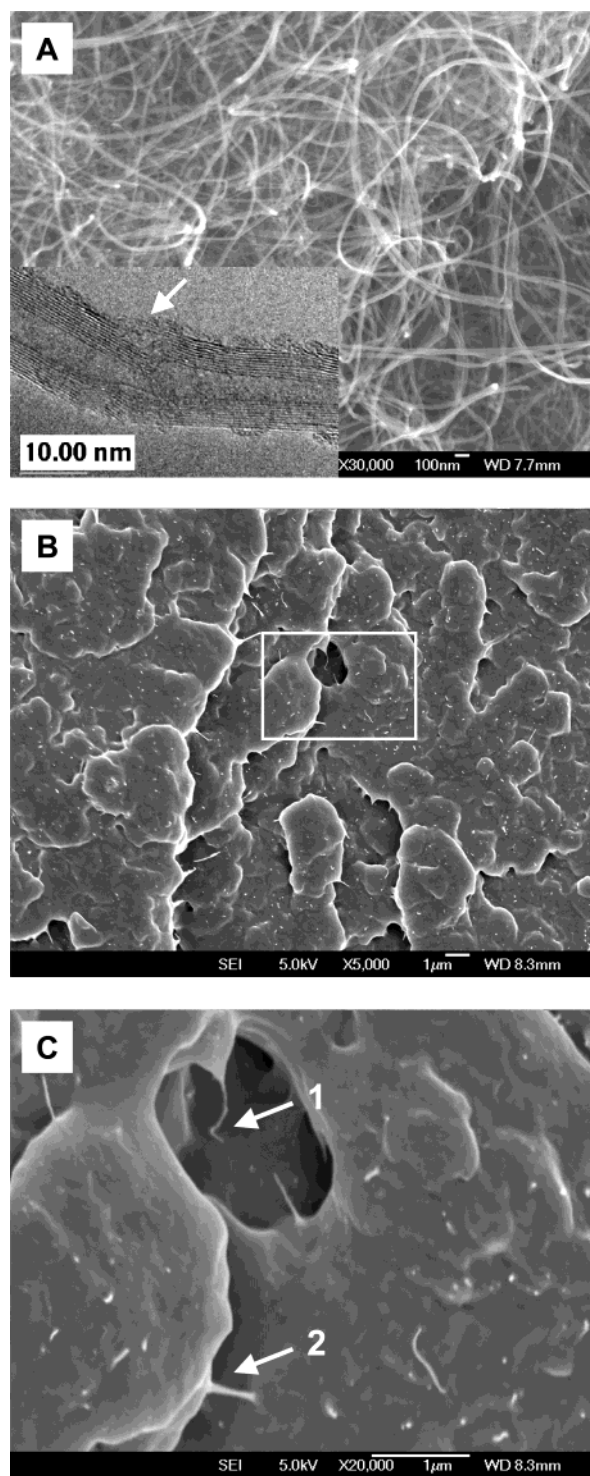


Figure 1. (A) Typical SEM image showing the morphology of MWNTs. The inset is a TEM image to illustrate the fine structure of MWNTs at higher magnification. (B) SEM image showing an overall morphology of failure surface for PA6 nanocomposite containing 1 wt % MWNTs. (C) Enlarged morphology of selected region in (B).

between MWNTs and nylon-6 matrix. The detailed reinforcing mechanism(s) resulting from CNTs is still under investigation. It is worth comparing the mechanical properties of PA6/MWNTs composites prepared here with those of PA6/clay nanocomposites reported in the literature. Upon incorporating 4.7 wt % montmorillonite into PA6 matrix, the tensile modulus and strength are only improved by about 68% and 42%, respectively.³⁸ Thus, the advantages and uniqueness of using the CNTs

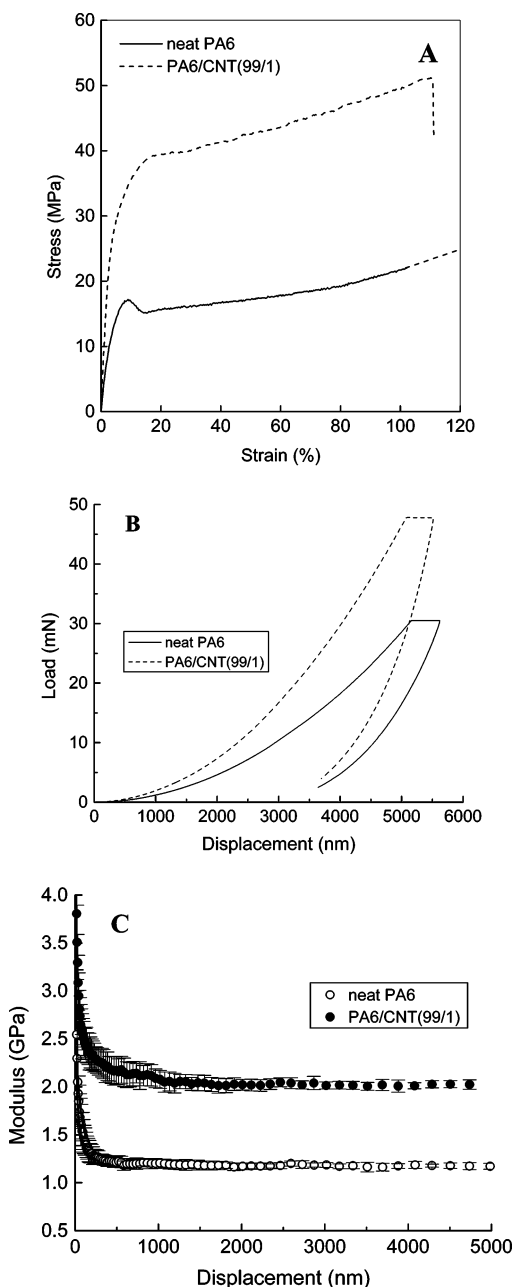


Figure 2. (A) Typical stress–strain curves. (B) Typical loading–unloading curves. (C) Modulus profiles as a function of displacement into sample surfaces for neat PA6 and its nanocomposite containing 1 wt % MWNTs.

Table 1. Summary of Mechanical Properties of Neat PA6 and Its Nanocomposite Containing 1 wt % Multiwalled Carbon Nanotubes

	neat PA6	PA6/MWNTs (99/1) composite
tensile modulus (MPa)	396.0 ± 36.6	852.4 ± 77.0
tensile strength (MPa) ^a	18.0 ± 2.2	40.3 ± 3.1
elongation at break (%)	> 150	125 ± 8
modulus ^b (GPa)	1.18 ± 0.02	2.02 ± 0.02
hardness (GPa)	0.06 ± 0.001	0.1 ± 0.002

^a Strength at yield. ^b Modulus obtained from nanoindentation tests.

as reinforcing nanofillers to make polymer nanocomposites are obvious.

Figure 2B shows typical loading–holding–unloading curves for neat PA6 and its composite containing 1 wt % MWNTs. It is immediately clear that the mechanical

response of neat PA6 and the composite differs considerably. Compared with that of neat PA6, the loading and unloading curve of the composite dramatically shifts upward, indicating a significant increase in stiffness of the material. However, the creep for the two samples at maximum holding segments show no distinct difference, probably indicating that MWNTs has little effect on the viscoelastic property of the PA6 matrix. Figure 2C shows the modulus profiles as a function of displacement into sample surfaces for neat PA6 and its composite containing 1 wt % MWNTs. After indentation depth approached 200 nm, the profile shows stable trends for both samples, indicating that MWNTs are homogeneously dispersed along the indentation direction at least until 5000 nm. Clearly, the addition of only 1 wt % MWNTs greatly improves the modulus (obtained from nanoindentation) by about 70% and the hardness by about 67% (Table 1). The results of *H* and *E* in Table 1 are averaged values in the depth between 4000 and 5000 nm.

With addition of only 1 wt % MWNTs into the PA6 matrix, the mechanical properties of the formed composite increase significantly. The high performance of the composite is attributed to homogeneous dispersion of MWNTs in the matrix as well as the strong interfacial interaction between MWNTs and polymeric matrix. As shown in Figure 1A, the MWNTs prepared and post-treated in our laboratory are loosely accumulated with large volume. They are quite different from those prepared by arc discharge which are usually densely aggregated with much higher compactness. Loose accumulation will benefit for the dispersion of MWNTs in the polymeric matrix without further ultrasonication. It is known that the ultrasonic treatment will result in the damage of the MWNTs,³⁹ thus affecting the mechanical strength of the MWNTs/polymer composites. Furthermore, the MWNTs synthesized by CVD followed by acid treatment contain many defects and –COOH groups.³⁴ Although the defects are disadvantageous to the mechanical strength of the MWNTs themselves, upon incorporating with polymeric matrix the presence of the defects and the functional groups increases the anchoring (or interacting) sites along the tubes with polymeric matrix, thus being favorable to stress transfer from polymer to CNTs. The hydrophilic functional groups on the MWNTs are helpful for improving the interaction with PA6, which possesses polar –CONH– groups along the polymer chains.¹⁷ Therefore, the compatibility and strong interaction between the MWNTs fillers and the matrix greatly enhances the dispersion as well as the interfacial adhesion, thus strengthening the overall mechanical performance of the composite.

In conclusion, MWNTs/PA6 nanocomposites have been prepared with enhanced overall mechanical properties by simple melt-compounding. Mechanical tests show that, compared with neat PA6, the tensile modulus, the tensile strength, and the hardness of the composite are greatly improved by about 115%, 120%, and 67%, respectively, with incorporating only 1 wt % MWNTs. SEM observation of the fracture surfaces of the composite indicates that a homogeneous dispersion of MWNTs throughout PA6 matrix and a strong interfacial adhesion between MWNTs and the matrix have been successfully achieved, which are responsible for the significant enhancements in mechanical properties. Detailed studies on the effect of addition of MWNTs on crystalline structure (morphology) and mechanical prop-

erties (such as fracture and strengthening mechanisms) of nylon-6 are still in progress.

References and Notes

- (1) Saito, R.; Dresselhouse, G.; Dresselhouse, M. S. *Physical Properties of Carbon Nanotubes*; Imperial College Press: London, 1998.
- (2) Ajayan, P. M.; Stephan, O.; Colliex, C.; Trauth, D. *Science* **1994**, *265*, 1212–1214.
- (3) Ajayan, P. M.; Schadler, L. S.; Giannaris, C.; Rubio, A. *Adv. Mater.* **2000**, *12*, 750–753.
- (4) Dalton, A. B.; Collins, S.; Muñoz, E.; Razal, J. M.; Ebron, V. H.; Ferraris, J. P.; Coleman, J. N.; Kim, B. G.; Baughman, R. H. *Nature (London)* **2003**, *423*, 703–703.
- (5) Ago, H.; Petritsch, K.; Shaffer, M. S. P.; Windle, A. H.; Friend, R. H. *Adv. Mater.* **1999**, *11*, 1281–1285.
- (6) Kymakis, E.; Alexandrou, I.; Amaratunga, G. A. J. *J. Appl. Phys.* **2003**, *93*, 1764–1768.
- (7) Goh, H. W.; Goh, S. H.; Xu, G. Q.; Lee, K. Y.; Yang, G. Y.; Lee, Y. W.; Zhang, W. D. *J. Phys. Chem. B* **2003**, *107*, 6056–6062.
- (8) Watts, P. C. P.; Hsu, W. K.; Kroto, H. W.; Walton, D. R. M. *Nano Lett.* **2003**, *3*, 549–553.
- (9) Barrau, S.; Demont, P.; Peigney, A.; Laurent, C.; Lacabanne, C. *Macromolecules* **2003**, *36*, 5187–5194.
- (10) Liao, K.; Li, S. *Appl. Phys. Lett.* **2001**, *79*, 4225–4227.
- (11) Zhu, J.; Kim, J. D.; Peng, H.; Margrave, J. L.; Khabashesku, V. N.; Barrera, E. V. *Nano Lett.* **2003**, *3*, 1107–1113.
- (12) Mitchell, C. A.; Bahr, J. L.; Arepalli, S.; Tour, J. M.; Krishnamoorti, R. *Macromolecules* **2002**, *35*, 8825–8830.
- (13) Satishkumar, B. C.; Govindaraj, A.; Mofokeng, J.; Subbanna, G. N.; Rao, C. N. R. *J. Phys. D: Appl. Phys.* **1996**, *29*, 4925–4934.
- (14) Kuznetsova, A.; Mawhinney, D. B.; Naumenko, V.; Yates, J. T., Jr.; Liu, J.; Smalley, R. E. *Chem. Phys. Lett.* **2000**, *321*, 292–296.
- (15) Ebbsen, T. W.; Hiura, H.; Bischer, M. E. *Adv. Mater.* **1996**, *8*, 155–160.
- (16) Jang, J.; Bae, J.; Yoon, S. H. *J. Mater. Chem.* **2003**, *13*, 676–681.
- (17) Lin, Y.; Hill, D. E.; Bentley, J.; Allard, L. F.; Sun, Y. P. *J. Phys. Chem. B* **2003**, *107*, 10453–10457.
- (18) Koshio, A.; Yudasaka, M.; Zhang, M.; Iijima, S. *Nano Lett.* **2001**, *1*, 361–363.
- (19) Shaffer, M. S. P.; Windle, A. H. *Adv. Mater.* **1999**, *11*, 937–941.
- (20) Qian, D.; Dickey, E. C.; Andrews, R.; Rantell, T. *Appl. Phys. Lett.* **2000**, *76*, 2868–2870.
- (21) Safadi, B.; Andrews, R.; Grulke, E. A. *J. Appl. Polym. Sci.* **2002**, *84*, 2660–2669.
- (22) Pirlot, C.; Willems, I.; Fonseca, A.; Nagy, J. B.; Delhalle, J. *Adv. Eng. Mater.* **2002**, *4*, 109–114.
- (23) Andrews, R.; Jacques, D.; Minot, M.; Randell, T. *Macromol. Mater. Eng.* **2002**, *287*, 395–403.
- (24) Potschke, P.; Fornes, T. D.; Paul, D. R. *Polymer* **2002**, *43*, 3247–3255.
- (25) Viswanathan, G.; Chakrapani, N.; Yang, H.; Wei, B.; Chung, H.; Cho, K.; Ryu, C. Y.; Ajayan, P. M. *J. Am. Chem. Soc.* **2003**, *125*, 9258–9259.
- (26) Wu, W.; Zhang, S.; Li, Y.; Li, J.; Liu, L.; Qin, Y.; Guo, Z. X.; Dai, L.; Ye, C.; Zhu, D. *Macromolecules* **2003**, *36*, 6286–6288.
- (27) Gong, X.; Liu, J.; Baskaran, S.; Voise, R. D.; Young, J. S. *Chem. Mater.* **2000**, *12*, 1049–1052.
- (28) Wagner, H. D.; Lourie, O.; Feldman, Y.; Tenne, R. *Appl. Phys. Lett.* **1998**, *72*, 188–190.
- (29) Bower, C.; Rosen, R.; Jin, L.; Han, J.; Zhou, O. *Appl. Phys. Lett.* **1999**, *74*, 3317–3319.
- (30) (a) Jia, Z.; Xu, C.; Liang, J.; Wei, B.; Wu, D.; Zhu, C. *Xinxiang Tan Cailiao* **1999**, *14*, 32–36. (b) Jia, Z.; Wang, Z.; Xu, C.; Liang, J.; Wei, B.; Wu, D.; Zhang, Z. *Qinghua Daxue Xuebao, Ziran Kexueban* **2000**, *40*, 14–16.
- (31) Bacsá, R. R.; Laurent, C.; Peigney, A.; Bacsá, W. S.; Vaugien, T.; Rousset, A. *Chem. Phys. Lett.* **2000**, *323*, 566–571.
- (32) Flahaut, E.; Peigney, A.; Laurent, C.; Rousset, A. *J. Mater. Chem.* **2000**, *10*, 249–252.
- (33) Zhang, W. D., unpublished material.
- (34) Goh, H. W.; Goh, S. H.; Xu, G. Q.; Pramoda, K. P.; Zhang, W. D. *Chem. Phys. Lett.* **2003**, *379*, 236–241.
- (35) Lucas, B. N.; Oliver, W. C.; Swindeman, J. E. *Mater. Res. Soc. Symp. Proc.* **1998**, *522*, 3–14.
- (36) Oliver, W. C.; Pharr, G. M. *J. Mater. Res.* **1992**, *7*, 1564–1583.
- (37) Liu, T. X.; Liu, Z. H.; Ma, K. X.; Shen, L.; Zeng, K. Y.; He, C. B. *Compos. Sci. Technol.* **2003**, *63*, 331–337.
- (38) Kojima, Y.; Usuki, A.; Kawasumi, M.; Okada, A.; Fukushima, Y.; Kurauchi, T.; Kamigaito, O. *J. Mater. Res.* **1993**, *8*, 1185–1189.
- (39) Lu, K. L.; Lago, R. M.; Chen, Y. K.; Green, M. L. H.; Harris, P. J. F.; Tsang, S. C. *Carbon* **1996**, *34*, 814–816.

MA035594F